Ion-mixing-induced amorphization in an immiscible Au - Mo system with a small size difference

1996 J. Phys.: Condens. Matter 8 383

(http://iopscience.iop.org/0953-8984/8/4/005)

J. Phys.: Condens. Matter **8** (1996) 383–388. Printed in the UK

Ion-mixing-induced amorphization in an immiscible Au–Mo system with a small size difference

F Pan†‡ and B X Liu†‡

† Department of Materials Science and Engineering, Tsinghua University, Beijing 100084, People's Republic of China

‡ Centre of Condensed Matter and Radiation Physics, China Centre of Advanced Science and Technology (World Laboratory), Beijing 100080, People's Republic of China

Received 22 September 1995

Abstract. Amorphization in immiscible Au–Mo multilayered films with a very small atomic size difference was achieved by 200 keV xenon ion mixing at 77 K. The experimental results revealed that Au/Mo multilayered films can be amorphized in the Mo content range 75–85 at.% upon ion mixing. Thermodynamically, the excess interfacial free energy stored in multilayered films was responsible for the formation of amorphous alloys.

1. Introduction

Amorphous materials are expected to have novel properties in many aspects, because of their non-crystalline structure containing no vulnerable grain boundaries. Since the first amorphous alloy obtained by rapid quenching of the melt in 1960 [1], various techniques have been developed to produce new amorphous materials, such as physical vapour deposition, laser quenching, ion implantation and solid state reaction (SSR) [2, 3]. In the last two decades, ion-beam mixing (IM) has been used as a powerful means to produce amorphous alloys and to study the amorphization mechanism of the binary systems [4]. On the basis of the extensive experimental data so far obtained, it has been commonly recognized that, in metal–metal systems, there is good correlation of the amorphous-alloy-forming ability in IM with thermodynamic and structural properties of the material systems, i.e. amorphous phase formation tends to occur in systems with large negative heats (ΔH_m) of mixing and large size differences [5]. Here the large negative ΔH_m between the constituents was the thermodynamic driving force for the formation of amorphous alloys during IM, and the large size mismatch prevented the formation of the simple structured solid solution competing against amorphization. It is naturally deduced that an amorphous alloy would not form in a binary system with a positive ΔH_m and with a small size difference, as the free-energy curve of the amorphous alloy phase is convex in shape and always higher than that of the two crystalline metals.

Recently, amorphous alloys have been formed in several systems with positive ΔH_m, e.g. Zr–Nd [6], Cu–Ta [7, 8], Au–Ru [9], Au–W [9] and Y–Mo [10]. In our recent study, it was also found that the Fe–Cu [11, 12] and Au–Ta [13] systems with a very small atomic size difference can be amorphized by IM and SSR, respectively. The above observation indicated that both a negative heat of mixing and a large atomic difference are not the only essential conditions for amorphization. Thus, an investigation of the thermodynamic

0953-8984/96/040383+06$19.50

and kinetic conditions of amorphization in binary metal systems with a positive ΔH_m and a small size difference is interesting and needed. This study was therefore dedicated to investigating the possibility of amorphous phase formation in the Au–Mo system by IM which has a positive $\Delta H_m = +5$ kJ mol^{-1} and a small size difference ($R_{\mathrm{Mo}}/R_{\mathrm{Au}} = 0.95$).

2. Experimental procedure

The Au/Mo multilayered samples were prepared by depositing alternately pure (99.99%) molybdenum and pure (99.99%) gold at rates of 0.1–0.2 nm s^{-1} onto a NaCl single-crystal substrate (with a freshly cleaved surface) in an electron-gun evaporation system with a vacuum of 5×10^{-7} Torr. The total thickness of the films was about 40 nm. Each Au/Mo multilayer system consisted of nine molybdenum layers and nine gold layers, i.e. the modulation wavelengths of the Au/Mo multilayers were about 4.4–4.5 nm, and the first layer on the substrate was molybdenum. Five stoichiometries were selected to carry out the IM experiment, i.e. alloys with 30, 60, 75, 85 and 92 at.% Mo. The relative layer thicknesses of their films were Au(3.2 nm)/Mo(1.3 nm), Au(1.9 nm)/Mo(2.6 nm), Au(1.2 nm)/Mo(3.3 nm), Au(0.7 nm)/Mo(3.7 nm) and Au(0.4 nm)/Mo(4.0 nm), respectively. The composition of the films was controlled by adjusting the relative layer thicknesses of constituent metals and were later confirmed by energy-dispersive spectroscopy (EDS) and Rutherford back-scattering (RBS) analysis within an experimental error of 5%. After deposition, the deposited films were then irradiated with 200 keV xenon ions at 77 K at doses ranging from 5×10^{14} to 1×10^{16} Xe^+ cm^{-2} in an implanter with a vacuum level of the order of 10^{-4} Pa. During irradiation, the ion-beam current density was controlled to be less than 1 μA cm^{-2}. The NaCl substrates were dissolved with deionized water and the metal films were held onto Cu grids. The structural and morphological changes of the samples were analysed by selected-area electron diffraction (SAD) and bright-field examination. The camera constant of the transmission electron microscopy (TEM) SAD was calibrated by x-ray diffraction results.

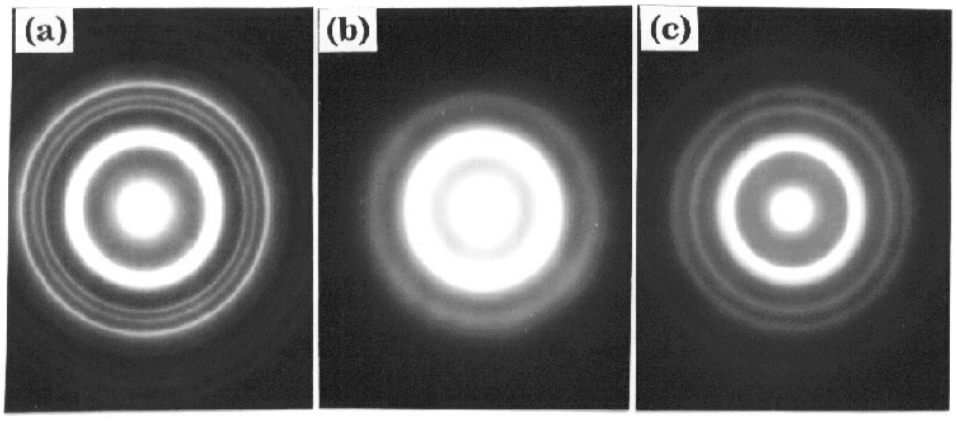

Figure 1. Typical TEM SAD patterns of $Au_{25}Mo_{75}$ multilayered films: (a) as deposited film; (b) film formed by IM by 200 keV xenon ions at a dose of 7×10^{14} Xe^+ cm^{-2}; (c) film formed by IM by 200 keV xenon ions at a dose of 5×10^{15} Xe^+ cm^{-1}.

3. Results and discussion

Figure 1(a) is a typical SAD pattern of the as-deposited $Au_{25}Mo_{75}$ multilayers, i.e. the $[Au(1.2\ nm)/Mo(3.3\ nm)]_9$ films (the subscript indicates the number of Au/Mo bilayers and is used similarly hereafter), showing the crystalline structure of Au and Mo metals. The as-deposited samples were then irradiated with 200 keV xenon ions at 77 K. The electron diffraction patterns of all the irradiated samples revealed that microstructural changes took place in the samples on increase in the irradiation dose. The $Au_{25}Mo_{75}$ multilayered films were partially amorphized at a dose of 5×10^{14} Xe^+ cm^{-2} and, when they were irradiated at a dose of 7×10^{14} Xe^+ cm^{-2}, the SAD pattern showed that the films had been completely amorphized. Figure 1(b) exhibits typical SAD patterns of the $Au_{25}Mo_{75}$ amorphous phases formed by 200 keV xenon IM at a dose of 7×10^{14} Xe^+ cm^{-2}. When the films were further irradiated at a dose of 5×10^{15} Xe^+ cm^{-2}, each amorphous halo changed into two separate haloes and diffration lines of FCC Au appeared in the SAD pattern shown in figure 1(c), indicating that the amorphous phase formed by IM transformed back to crystalline phases. $Au_{15}Mo_{85}$ ($[Au(0.7\ nm)/Mo(3.7\ nm)]_9$) multilayers were also completely amorphized at a dose of 1×10^{15} Xe^+ cm^{-2} and the amorphous $Au_{15}Mo_{85}$ cannot be crystallized even when the dose was higher than 2×10^{16} Xe^+ cm^{-2}. Figure 2 shows the SAD pattern of the amorphous $Au_{15}Mo_{85}$. For the $Au_{40}Mo_{60}$ ($[Au(1.9\ nm)/Mo(2.6\ nm)]_9$) films, the sample could not be completely amorphized by IM. On the Au-rich side, the $Au_{70}Mo_{30}$ ($[Au(1.9\ nm)/Mo(2.6\ nm)]_9$) films transformed into an Au-based solid solution with FCC structure upon xenon IM and, on the Mo-rich side, the terminal solid solution also formed in the Au_8Mo_{92} ($[Au(1.9\ nm)/Mo(2.6\ nm)]_9$) films by IM, indicating that the IM can increase the solid solubility between Au and Mo. Table 1 lists the phase changes of the Au–Mo multilayers upon 200 keV xenon IM at various doses at 77 K. One sees clearly that amorphization can be achieved in some multilayered films in the immiscible Au–Mo system with a small atomic size difference by IM. The Mo content range obtained for amorphization by IM was around 75–85 at.%.

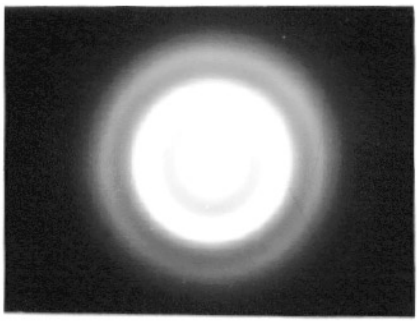

Figure 2. The typical SAD pattern of amorphous $Au_{15}Mo_{85}$ formed by 200 keV xenon IM at a dose of 5×10^{15} Xe^+ cm^{-2}.

To interpret the above observations, a free-energy diagram of the Au–Mo system was constructed on the basis of the model of Nissen *et al* [14] and the method proposed by Alonso and Simorar [15]. Figure 3 is the free-energy diagram calculated for the Au–Mo system at room temperature. From this figure, one can see that the free-energy curve of the amorphous phase is lower than those of the two terminal solid solutions within a narrow Mo content range 75–90 at.%. Simply taking this range as a measure of the glass-forming

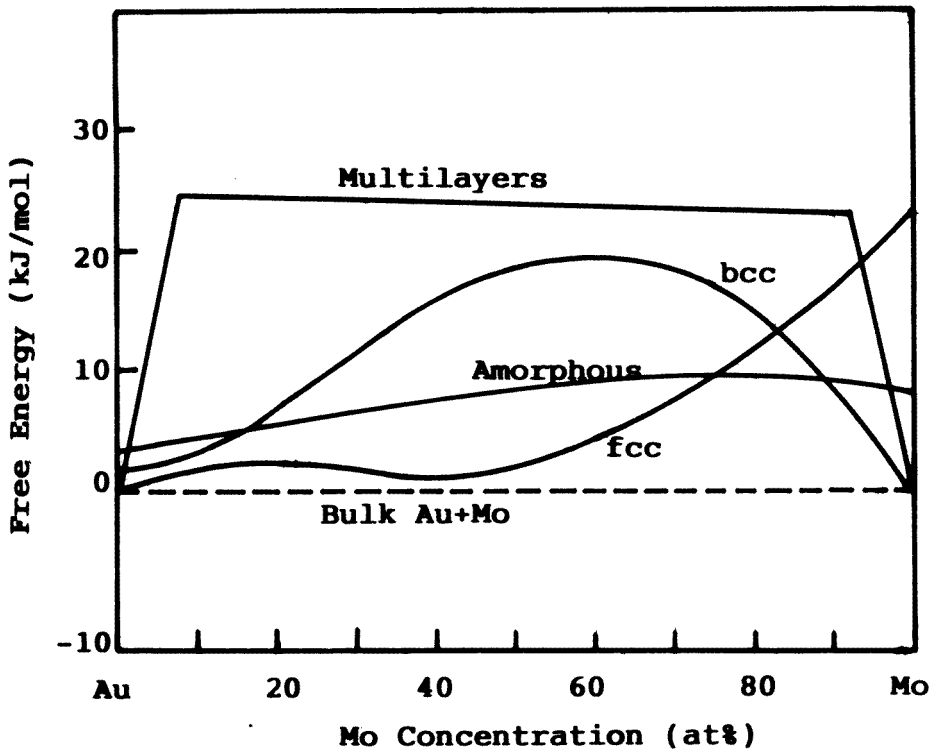

Figure 3. The calculated free-energy diagram of the Au–Mo system.

Table 1. Amorphization in Au–Mo multilayers by IM: A, completely amorphized; PA partially amorphized.

Dose (10^{14} Xe^+ cm^{-2})	Amorphization in the following				
	$Au_{70}Mo_{30}$	$Au_{40}Mo_{60}$	$Au_{25}Mo_{75}$	$Au_{15}Mo_{85}$	Au_8Mo_{92}
As deposited	Au+Mo	Au+Mo	Au+Mo	Au+Mo	Au+Mo
5	Au	Au+A	PA	PA	Mo
7	Au	Au+A	A	PA	Mo
10	Au	Au+A	A	A	Mo
30	Au	Au+A	PA	A	Mo
50	Au	Au+A	A+Au	A	Mo

ability, the Mo content range favouring amorphization for the Au–Mo system is therefore from 75 to 90 at.%, which is in good agreement with the narrow Mo content range revealed by IM experiments. Therefore, the free-energy calculation can serve as a semi-experimental explanation for amorphization in the Au–Mo system.

From figure 3, one can also see that the free energy of the amorphous phase and the two terminal solid solutions is always higher than that of the ground state of a mixture of Au and Mo crystalline phases. How can we explain the physical mechanism of IM amorphization in a binary metal system with a positive heat of mixing? It has been commonly recognized

that the thermodynamic driving force for amorphous alloys with a positive heat of mixing was provided by some non-equilibrium processes, because it has been estimated that the effective cooling rate can be as high as 10^{13}–10^{14} K s^{-1} in the IM process; IM can produce many defects in the films and thus enhance the diffusion for formation of the amorphous phase, etc. So far, many possible models have been proposed for the formation of the amorphous phase, e.g., ballistic mixing, thermal spike models, radiation-enhanced diffusion and radiation-induced segregation. These hypotheses agree fairly well with many of the experimental results. However, these hypotheses are not entirely successful, and several examples exist for a metastable phase transformed to stable phase upon IM; for example, in our experiment, when the $Au_{25}Mo_{75}$ amorphous films were further irradiated at a dose of 5×10^{15} Xe^{+} cm^{-2}, the amorphous phase formed by IM transformed back to crystalline phases. Since all the observed amorphization upon IM took place in multilayered films consisting of a certain number of interfaces, which should have played some role, yet this has been omitted in previous studies. It is known that the atoms at the interfaces are in a metastable configuration and thus possess a higher free energy than those in the bulk [16], and the influence of the interfacial free energy stored in the multilayered films should be evaluated [10]. Following the well documented literature [10], the free energy of the Au–Mo multilayered films with 17 interfaces (the total thickness of the film is 40 nm) was calculated and the free-energy curve of the multilayers was added to figure 3. Thus, from this figure, one can see that the free-energy curves of the amorphous phase and two terminal solid solutions are lower than that of the as-deposited multilayered films, which can provide the thermodynamic driving force for the amorphous phase transformation. Therefore, it can be thought that the interfacial free energy may be one of the main thermodynamic driving forces for the formation of the amorphous phase.

4. Conclusion

In summary, we have shown the amorphization of Au–Mo multilayers with very small atomic size difference upon IM. Whether the amorphous phase formed or not in a binary metal system depends on the thermodynamically and kinetically competing results of various equilibrium phases, non-equilibrium crystalline phases and amorphous phase.

Acknowledgments

This work was supported in part by the National Natural Science Foundation of China and by the Administration of Tsinghua University.

References

[1] Duwez P, Willens R H and Klement W 1960 *J. Appl. Phys.* **31** 1136
[2] Schwarz R B and Johnson W L 1983 *Phys. Rev. Lett.* **51** 415
[3] Lau S S, Liu B X and Nicolet M A 1983 *Nucl. Instrum. Methods* **209–10** 97
[4] Liu B X 1989 *Nucl. Instrum. Methods* B **40–1** 603
[5] Giessen B C 1982 *Proc. 4th Int. Conf. on Rapidly Quenched Metals (Sendai, 1981)* (Sendai: Japan Institute of Metals) p 213
[6] Jin O and Liu B X 1994 *J. Phys.: Condens. Matter* **6** L39
[7] Tsaur Y 1980 *Thesis* California Institute of Technology
[8] Sakurai K, Yamada Y, Lee C H, Fukunaga T and Mizutani U 1990 *Appl. Phys. Lett.* **57** 2660
[9] Meissener J, Kopitzki K, Mertler G and Peiner E 1987 *Nucl. Instrum. Methods* B **19–20** 699
[10] Zhang Z J, Jin O and Liu B X 1995 *Phys. Rev.* B **51** 8076

[11] Huang L J and Liu B X 1990 *Appl. Phys. Lett.* **57** 1402
[12] Pan F, Tao K, Yang T and Liu B X 1994 *Phys. Status Solidi* **142** K33
[13] Pan F, Chen Y G and Liu B X 1995 *Appl. Phys. Lett.* **67** 780
[14] Niessen A K, Miedema A R, de Boeer F R and Boom R 1988 *Physica* B **151** 401
[15] Alonso J A and Simozar S 1983 *Solid State Commun.* **46** 765
[16] Clemens B M and Hufnagel T C 1993 *J. Alloy Compounds* **194** 221